Application of a time-convolutionless stochastic Schrödinger equation to energy transport and thermal relaxation

R. Biele[1,2], C. Timm[2] and R. D'Agosta[1,3]

[1]ETSF Scientific Development Center, Departamento de Física de Materiales, Universidad del País Vasco, E-20018 San Sebastián, Spain

[2]Institute of Theoretical Physics, Technische Universität Dresden, D-01062 Dresden, Germany

[3]IKERBASQUE, Basque Foundation for Science, E-48011, Bilbao, Spain

Abstract. Quantum stochastic methods based on effective wave functions form a framework for investigating the generally non-Markovian dynamics of a quantum-mechanical system coupled to a bath. They promise to be computationally superior to the master-equation approach, which is numerically expensive for large dimensions of the Hilbert space. Here, we numerically investigate the suitability of a known stochastic Schrödinger equation that is local in time for the description of thermal relaxation and energy transport. This stochastic Schrödinger equation can be solved with a moderate numerical cost, indeed comparable to that of a Markovian system, but reproduces the dynamics of a system evolving according to a general non-Markovian master equation. After verifying that it describes thermal relaxation correctly, we apply it for the first time to the energy transport in a spin chain. We also discuss a portable algorithm for the generation of the coloured noise associated with the numerical solution of the non-Markovian dynamics.

1. Introduction

Stochastic methods applied to the investigation of the dynamics of physical systems coupled to external baths have a long history dating back to Einstein [1] and Langevin [2]. The idea behind these approaches is that the many degrees of freedom of the bath induce random motion in the system [3–8]. Classically, this stochastic motion is due to collisions between the particles of the system and of the bath and can be described by a Langevin equation for certain system variables. Quantum mechanically, the randomness is introduced by transitions between different states of the system induced by the bath and can be described by a stochastic Schrödinger equation (SSE) [7, 9–13]. Alternatively, one can derive statistical descriptions averaging over many realisations of the stochastic process, leading to the Fokker-Planck equation for the distribution function of a classical system and the master equation for the reduced density operator of a quantum system [3–8], respectively. Assuming the equivalence between the master equation for the density matrix $\hat{\rho}(t)$ and the SSE [7, 12], which might not always hold [14], the latter has sometimes been seen as a "quick and dirty" way to obtain the solution of the former. Indeed, the numerical solution of the master equation scales poorly with the number of states kept in the calculation since it is an equation of motion for a *matrix* in state space, whereas a Schrödinger equation is an equation for a *vector*. This strongly limits the applicability of the master equation to complex systems. In particular, if the quantum system consists of interacting particles, in which case the state space is the Fock space, the scaling of the density matrix restricts the range of system that could be tackled with numerical calculations and approximate methods are needed [15]. Alternatively, one can establish a time-dependent density functional theory [16] of open quantum systems [14, 17, 18].

In general, the dynamics of an open system is non-Markovian, i.e., the change of the state of the system at a certain time does not only depend on its present state but also on its state at all previous times. Understandably, the solution of a non-Markovian master equation [19, 20] is difficult because it involves the evaluation of a convolution integral which depends on the history of the system. Therefore, one often employs a Markov approximation, which replaces the dynamical memory kernel in this convolution integral by a δ-function in time. In doing so, however, one looses the connection with the exact dynamics and the ability to reproduce the correct steady state, unless one is capable of constructing effective bath-system operators that recover the exact behaviour [21]. It should be noted that an exact time-convolutionless master equation can be derived [5, 22–24]. However, this does not usually reduce the numerical complexity since one needs to evaluate the generator of the time-convolutionless master equation describing the history of the system at each time step of the numerical integration.

In order to study the non-Markovian dynamics it would be advantageous to have a SSE that is local in time but is nevertheless able to reproduce the dynamics induced by a non-Markovian master equation (NMME). Such an equation has been proposed by Strunz and coworkers: first mentioned as a byproduct in [25], it has been applied to the spin-boson model and compared to non-linear SSEs in [26] and also to a more realistic two-level

model immersed in a photonic band-gap material in [27]. Here, we arrive at the same time-convolutionless SSE (TCLSSE) of Strunz and coworkers starting from a non-Markovian SSE obtained by Gaspard and Nagaoka [11]. We show how the dynamics induced by the TCLSSE and the NMME coincide up to third order in the coupling parameter between the system and the bath.

A promising application of the formalism is the investigation of the bath-induced energy transport in the system. For this the system is coupled locally at its ends to two baths kept at different temperatures. The temperature gradient induces a thermal force leading to energy transport in the system. Before investigating this non-equilibrium situation within the TCLSSE approach, we will first test whether the TCLSSE is able to reproduce relaxation dynamics correctly: In contact with a single bath at a constant temperature, the system should approach an equilibrium state with that temperature. It can be shown that in the non-Markovian case there exists an exact condition that the memory kernel must satisfy for the system to reach thermal equilibrium, i.e., $\hat{\rho}(t \to \infty) \propto \exp(-\beta \hat{H})$ [5, 28]. ‡ This condition is known as *detailed balance* since it relates the absorption and emission probabilities. The detailed-balance condition is usually no longer satisfied if the Markov approximation is made [5, 28]. Hence, the history dependence of the equation of motion is an essential ingredient for thermal relaxation. This begs the question of whether a TCLSSE is also able to correctly describe thermal relaxation dynamics. To answer this question, we study the relaxation of a simple three-level system employing the TCLSSE and compare its dynamics to the one obtained from the NMME. This rather pedagogical study verifies the applicability of the TCLSSE to thermal transport, where we study for the first time the non-Markovian time evolution of the energy current induced by a thermal gradient.

The numerical solution of the TCLSSE requires the generation of complex coloured noise to mimic the correlation functions of the non-Markovian baths [29]. Here we introduce a portable and fast algorithm to generate any coloured noise whose power spectrum is a positive function. The algorithm relies on the ability of performing a fast Fourier transform and is therefore easily optimised. Other algorithms have been presented in the past to generate real coloured noise [30–32]. In section 2.2, we compare our algorithm to some of them and show that it performs better than these routines while having a broader range of applicability.

‡ It is well known that the Hamiltonian $\hat{H}$ appearing here might be different from the one describing the system dynamics, due for example to the Stark and Lamb shifts. For simplicity, we here assume that these effects can be neglected, since they are normally proportional to λ^4, where λ is the coupling parameter between the system and the bath.

2. Method

2.1. A time-convolutionless stochastic Schrödinger equation

Our starting point is a standard second-order NMME [4, 5, 8, 19, 20]. The coupling between the system and the bath is taken to be bilinear,

$$\hat{H}_{\rm int} = \lambda \sum_a \hat{S}_a \otimes \hat{B}_a, \tag{1}$$

in the operators $\hat{S}_a$ and $\hat{B}_a$ from the system and the bath, respectively. If any operator of the system commutes or anticommutes with any operator of the bath, one can always expand any coupling operator in this form.

In the following we assume that the bath and the system do not exchange *fermions*, i.e., $\hat{S}_a$ and $\hat{B}_a$ commute with each other. We further restrict ourselves to the case that $\hat{S}_a$ and $\hat{B}_a$ are Hermitian operators; the extension to the more general case where only $\hat{H}_{\rm int}$ is Hermitian is straightforward. Under the assumptions of weak system-bath interaction, factorisation of the full density operator at the initial time $t = 0$ and vanishing averages of bath operators to first order, the equation of motion for the reduced density operator $\hat{\rho}$ of the system is given by [4, 5, 7, 8]

$$\frac{d\hat{\rho}(t)}{dt} = -i\big[\hat{H}, \hat{\rho}(t)\big] + \lambda^2 \sum_a [\hat{S}_a, \hat{M}_a^\dagger(t) - \hat{M}_a(t)], \tag{2}$$

up to second order in the coupling parameter λ. We have set $\hbar = 1$ and defined

$$\hat{M}_a(t) \equiv \sum_b \int_0^t d\tau\, c_{ab}(t,\tau)\, e^{-i\hat{H}(t-\tau)}\, \hat{S}_b\, \hat{\rho}(\tau)\, e^{i\hat{H}(t-\tau)}. \tag{3}$$

In this NMME, $\hat{H}$ is the Hamiltonian of the system and the correlation kernel is given by

$$c_{ab}(t,\tau) \equiv {\rm Tr}_B[\hat{\rho}_B^{\rm eq}\, \hat{B}_a(t)\, \hat{B}_b(\tau)], \tag{4}$$

where the trace is over the bath degrees of freedom, $\hat{B}_a(t) \equiv e^{i\hat{H}_B t}\hat{B}_a e^{-i\hat{H}_B t}$ and $\hat{H}_B$ is the Hamiltonian of the bath. Here, $\hat{\rho}_B^{\rm eq}$ is the statistical operator of the bath. If $\hat{\rho}_B^{\rm eq}$ describes a single bath in thermal equilibrium, $\hat{\rho}_B^{\rm eq} \propto \exp(-\beta\hat{H}_B)$, where β is the inverse temperature, the system should relax towards thermal equilibrium, $\hat{\rho}(t \to \infty) \propto \exp(-\beta\hat{H})$, with the same temperature as the bath. The property that if a steady state exists, it coincides with the state of thermal equilibrium must be encoded in the correlation kernel $c_{ab}(t,\tau)$. Indeed, one can show that the system relaxes towards thermal equilibrium if $c_{ab}(t,\tau) = c_{ab}(t-\tau)$ and the power spectrum $C_{ab}(\omega) \equiv \int_{-\infty}^{+\infty} dt\, c_{ab}(t)\, e^{-i\omega t}$ satisfies the detailed-balance condition [5, 28]

$$C_{ab}(-\omega) = e^{\beta\omega}\, C_{ba}(\omega). \tag{5}$$

Gaspard and Nagaoka [11] have shown that the dynamics introduced by the NMME can be obtained not only by a numerical integration of (2) but also by the solution of a SSE

for a state $|\Psi(t)\rangle$,

$$i\frac{d}{dt}|\Psi(t)\rangle = \hat{H}|\Psi(t)\rangle + \lambda\sum_a \gamma_a(t)\,\hat{S}_a|\Psi(t)\rangle \\ - i\,\lambda^2\sum_{a,b}\hat{S}_a\int_0^t dt'\,c_{ab}(t')\,e^{-i\hat{H}t'}\,\hat{S}_b|\Psi(t-t')\rangle. \tag{6}$$

In this non-Markovian SSE (NMSSE), the complex noises $\gamma_a(t)$ have the properties

$$\overline{\gamma_a(t)} = 0, \quad \overline{\gamma_a(t)\gamma_b(t')} = 0, \quad \overline{\gamma_a^*(t)\gamma_b(t')} = c_{ab}(t-t') \tag{7}$$

and one can obtain the dynamics of the open quantum system by taking the average over realisations of the stochastic process, indicated by the overline. In particular, the reduced density operator is obtained as $\hat{\rho}(t) = \overline{|\Psi(t)\rangle\langle\Psi(t)|}$. However, any attempt to solve the NMSSE (6) requires a large numerical effort due to the time integral, which needs to be evaluated at every time step and for every realization. This begs the question of whether there exists a simpler SSE that reproduces on average the dynamics induced by the NMME. This is the case, as Strunz and Yu have shown [25].

Indeed, the TCLSSE

$$i\frac{d}{dt}|\Psi(t)\rangle = \left(\hat{H} + \lambda\sum_a \gamma_a(t)\,\hat{S}_a - i\,\lambda^2\,\hat{T}(t)\right)|\Psi(t)\rangle \tag{8}$$

with

$$\hat{T}(t) \equiv \sum_{a,b}\hat{S}_a\int_0^t dt'\,c_{ab}(t')\,e^{-i\hat{H}t'}\,\hat{S}_b\,e^{i\hat{H}t'} \tag{9}$$

reproduces on average the dynamics induced by the NMME (2) up to third order in λ [25]. To prove this, we write (8) in the interaction picture, $|\Psi_I(t)\rangle = e^{i\hat{H}t}\,|\Psi(t)\rangle$ and $\hat{S}_a(t) = e^{i\hat{H}t}\hat{S}_a\,e^{-i\hat{H}t}$ and expand the time-evolution operator up to second order in λ,

$$|\Psi_I(t)\rangle \cong \Bigg[\mathbb{1} - i\lambda\sum_a\int_0^t dt_1\,\gamma_a(t_1)\,\hat{S}_a(t_1) \\ - \lambda^2\sum_{a,b}\int_0^t dt_1\int_0^{t_1} dt_2\,c_{ab}(t_2)\,\hat{S}_a(t_1)\,\hat{S}_b(t_1-t_2) \\ -\lambda^2\sum_{a,b}\int_0^t dt_1\int_0^{t_1} dt_2\,\gamma_a(t_1)\,\hat{S}_a(t_1)\,\gamma_b(t_2)\,\hat{S}_b(t_2)\Bigg]\,|\Psi_I(0)\rangle \\ + \mathcal{O}(\lambda^3). \tag{10}$$

This expansion is inserted into the expression for the reduced density operator $\hat{\rho}_I(t) = \overline{|\Psi_I(t)\rangle\langle\Psi_I(t)|}$. By performing the average, using the properties given in (7) and the identity

$c_{ab}(\tau,t) = c^*_{ba}(t,\tau)$, and differentiating with respect to t, we arrive at

$$\begin{aligned}\frac{d}{dt}\hat{\rho}_I(t) = \lambda^2 \sum_{a,b} \int_0^t d\tau \,\big[& c_{ab}(t,\tau)\, \hat{S}_b(\tau)\, \hat{\rho}_I(0)\, \hat{S}_a(t) \\ & - c_{ab}(t,\tau)\, \hat{S}_a(t)\, \hat{S}_b(\tau)\, \hat{\rho}_I(0) \\ & + c^*_{ab}(t,\tau)\, \hat{S}_a(t)\, \hat{\rho}_I(0)\, \hat{S}_b(\tau) \\ & - c^*_{ab}(t,\tau)\, \hat{\rho}_I(0)\, \hat{S}_b(\tau)\, \hat{S}_a(t)\big] + \mathcal{O}(\lambda^4). \end{aligned} \tag{11}$$

Note that the averages of the terms in λ^3 vanish. Furthermore, replacing $\rho_I(0)$ by $\rho_I(\tau) + \mathcal{O}(\lambda^2)$ does not change the equation up to terms of order λ^3. Finally, by returning to the Schrödinger picture we arrive at the NMME (2) up to terms of order λ^3, i.e., higher than the order up to which these equations are valid anyway. Indeed, the NMME and the SSE are usually derived as a second-order expansion in the coupling parameter λ. This is remarkable since one might expect a more complex time-non-local SSE to be required for reproducing the dynamics of the NMME (2). Still, the TCLSSE is local in time, i.e., the operator $\hat{T}(t)$ does not depend on the state of the system at previous times and can thus be calculated once before the numerical integration and be used for each realisation of the stochastic process. Hence, the numerical cost of solving each realisation of the TCLSSE is comparable to that of a Markovian SSE [7, 11].

We note that at the same level of approximation, λ^3, we can derive a time-convolutionless master equation instead of the non-local equation (2). Indeed, in (11) we could replace $\rho_I(0)$ by $\rho_I(t) + \mathcal{O}(\lambda^2)$, arriving at

$$\begin{aligned}\frac{d}{dt}\hat{\rho}_I(t) = \lambda^2 \sum_{a,b} \int_0^t d\tau \,\big[& c_{ab}(t,\tau)\, \hat{S}_b(\tau)\, \hat{\rho}_I(t)\, \hat{S}_a(t) \\ & - c_{ab}(t,\tau)\, \hat{S}_a(t)\, \hat{S}_b(\tau)\, \hat{\rho}_I(t) \\ & + c^*_{ab}(t,\tau)\, \hat{S}_a(t)\, \hat{\rho}_I(t)\, \hat{S}_b(\tau) \\ & - c^*_{ab}(t,\tau)\, \hat{\rho}_I(t)\, \hat{S}_b(\tau)\, \hat{S}_a(t)\big] + \mathcal{O}(\lambda^4). \end{aligned} \tag{12}$$

However, since in general we expect the density matrix and the operators $\hat{S}_a$ not to commute, the integral over τ still contains the density matrix in a complicated manner. From a numerical point of view, the solution of this equation is therefore not simpler than that of (2). The equivalence of (2) and (12) is a generalization of the result that a time-convolutionless Pauli master equation, i.e., a master equation for the diagonal components of the density matrix only, can be proven to be equivalent to a Nakajima-Zwanzig-Markov Pauli master equation to second order in λ [24, 33].

2.2. Generation of coloured noise

The TCLSSE requires the generation of coloured noise and thus the method will only be practicable if an efficient algorithm for the generation of this noise is available. Such an algorithm indeed exists, as we show below, where we extend an algorithm presented by Rice [30, 31] to the complex noise required here. We consider only a single bath operator; the generalisation to several bath operators is straightforward.

Some of the existing algorithms for the generation of coloured noise rely on the numerical solution of a stochastic differential equation that has to produce noise with the given target correlation function $c(t)$ [29, 34]. However, such an equation is a piece of information that is rarely available, since even the analytic expression for $c(t)$ may not be known. Except for a few simple models, it is more common to have access to the power spectrum $C(\omega) = \int_{-\infty}^{+\infty} dt\, c(t)\, e^{-i\omega t}$. Indeed, $C(\omega)$ is connected to the quantum transitions in the bath.

On the other hand, the algorithm presented in [32] does not require the knowledge of a stochastic differential equation. However, besides the power spectrum $C(\omega)$ is does require the inverse Fourier transform of its square root. This quantity is then convoluted with a white noise to generate the target real coloured noise. We will introduce an algorithm that directly uses $\sqrt{C(\omega)}$ as input, thereby reducing the numerical cost compared to the algorithm of [32] and that generates a complex coloured noise with the properties given in (7). Indeed, one can easily prove that the noise $\gamma(t)$ can be generated by

$$\gamma(t) = \int_{-\infty}^{+\infty} \frac{d\omega}{\sqrt{2\pi}} \sqrt{C(\omega)}\, x(\omega)\, e^{i\omega t}, \tag{13}$$

where $x(\omega)$ is a white-noise process in the frequency domain satisfying

$$\overline{x(\omega)} = 0, \quad \overline{x(\omega)x(\omega')} = 0, \quad \overline{x^*(\omega)x(\omega')} = \delta(\omega - \omega'). \tag{14}$$

By substituting (13) into $\overline{\gamma^*(t)\gamma(t')}$ and using (14), we immediately arrive at the third relation of (7). The other relations are proven in a similar way. From a numerical point of view, the generation of this coloured noise requires the calculation of the Fourier transform in (13). We discretize the frequency domain with the uniform step $\Delta\omega$, and generate $x(\omega)$ by using two independent gaussian random noises with zero mean and unitary variance, $N(0,1)$, therefore $x(\omega) = (N(0,1) + iN(0,1))/\sqrt{2\Delta\omega}$. A similar algorithm restricted to real coloured noise has been proposed in the past [30, 31].

In order to compare our algorithm with the two from [32] and [30,31], we choose a test function for which we know $c(t)$ and $C(\omega)$ analytically, namely $c(t) = (2\pi\sigma^2)^{-1/4} e^{-t^2/2\sigma^2}$ and $C(\omega) = (2\pi\sigma^2)^{1/4}\, e^{-\omega^2\sigma^2/2}$. We fix $\sigma = 1$ as our unit of time and choose the interval $t \in [-25, 25]$ for the numerical Fourier transform. To quantify the agreement between the target $c(t)$ and the noise generated by the three algorithms, we use the statistical variance $\delta_c = \int_{-\infty}^{+\infty} dt\, |c(t) - \overline{\gamma(0)\gamma^*(t)}|^2 / \int_{-\infty}^{+\infty} dt\, |c(t)|^2$. In principle, these algorithms produce an exact representation of the target correlation function. Discrepancies arise from the finite mesh on which the Fourier transform is evaluated, the finite number of independent realisations of the noise that we generate and the limitations of the white noise generation.

In figure 1, we report the variance δ_c as a function of the number of independent realisations of the noise. We see that the algorithm (13) performs better for a large number of runs (at least 2×10^5), while being close to the other two for a small number of runs. The algorithm proposed in [32] suffers from the need of performing a double Fourier transform, although for a large number of runs its performance improves consistently. On the other hand, we can consider the total computation time to generate a given number of realisations.

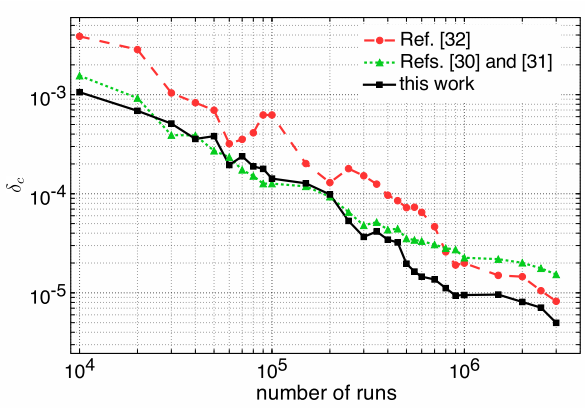

Figure 1. Statistical variance δ_c versus the number of independent realisations of the coloured noise, calculated using a 16384 point mesh in time and frequency. The red (dashed) line represents the optimised version of the algorithm presented in [32], the green (dotted) line the algorithm proposed by Rice [30, 31] and the black (solid) line the results obtained from (13).

Taking the time needed by algorithm (13) as a reference, the algorithm of [30, 31] is about 7% slower and the algorithm of [32] is about 50% slower. However, we stress that the main advantage of the algorithm (13) does not lie in the moderate numerical improvement but in the simplification it brings about by only requiring the power spectrum as input.

For illustration, we show in figure 2 a single realisation of the noise (13) with 16834 mesh points. Notice that due to the use of the fast Fourier transform, the noise is periodic over the simulation time.

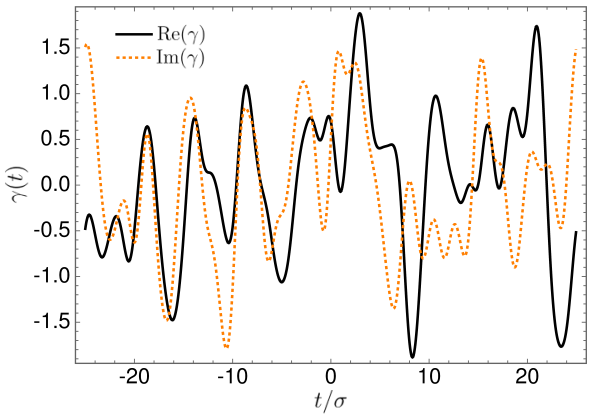

Figure 2. The real (black, continuous line) and imaginary (orange, dotted line) parts of a single realisation of the coloured noise, (13), for a mesh in time of 16384 points. The function $\gamma(t)$ appears smooth as a function of time due to the fact that time enters in $\gamma(t)$ via the oscillating term in the right hand side of (13). Similar behaviours are obtained with the other two algorithms.

2.3. Thermal relaxation of a three-level system

Here, we test whether the TCLSSE is capable to describe thermal relaxation dynamics correctly when connected to a single bath. This will then allow us to study energy transport within the TCLSSE approach in section 3.

We consider the coupling of an electronic system to the electromagnetic field in a three-dimensional cavity. In the dipole approximation, one can derive from first principles the power spectrum for this system (we set the speed of light to unity),

$$C_{\mathrm{cav}}(\omega) = \frac{|\omega|^3}{\pi\epsilon_0}\big[n_B(\beta|\omega|) + \theta(-\omega)\big] \quad \text{for} \quad |\omega| < \omega_c, \tag{15}$$

where $n_B(\beta\omega) \equiv 1/(e^{\beta\omega} - 1)$ is the Bose-Einstein distribution function, $\theta(\omega)$ is the Heaviside step function and ω_c is a cutoff frequency determined by the dimensions of the system. This cutoff is necessitated by the assumption made in the dipole approximation that the electromagnetic field is uniform in the region of space occupied by the system. The derivation of this power spectrum can be found in the appendix. For $|\omega| > \omega_c$, the power spectrum is set to vanish. Note that increasing ω_c does not change the relaxation dynamics as long as ω_c is larger than the energy differences in the system and hence does not exclude any transitions. One can show that the detailed-balance condition (5) is satisfied by this power spectrum. Since for this model system the correlation function $c(t)$ is not given in analytical form, we will use (13) to generate the noise.

In order to quantify the agreement between the noise generated by (13) and the power spectrum (15), we have performed a Fourier transform of the time-domain signal and compared it to our target. Figure 3 shows that the agreement is excellent.

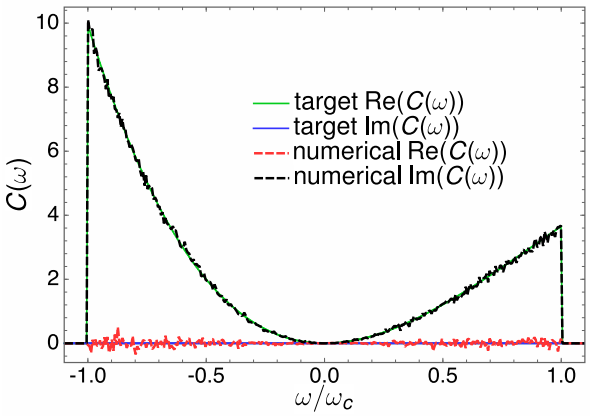

Figure 3. Comparison between the target, (15), (solid lines) and the Fourier transform of the correlation function obtained from (13) by averaging over 90 000 realisations of the noise (dashed lines).

For the electronic system we consider a three-site spinless tight-binding chain described by the Hamiltonian

$$\hat{H} = -T\left(\hat{c}_1^\dagger\hat{c}_2 + \hat{c}_2^\dagger\hat{c}_1 + \hat{c}_2^\dagger\hat{c}_3 + \hat{c}_3^\dagger\hat{c}_2\right), \tag{16}$$

where the operator $\hat{c}_i^\dagger$ creates an electron at site i, and assume a single electron to be present. This system is coupled to the electromagnetic field inside the cavity by the operator

$$\hat{S} = -q \sum_{i,j} \vec{u} \cdot \langle W_i | \vec{r} | W_j \rangle \, \hat{c}_i^\dagger \hat{c}_j, \tag{17}$$

where q is the charge of the electron and $|W_i\rangle$ is the single-particle state localized at site i. For simplicity, we assume that each relevant mode of the cavity has the same polarization direction $\vec{u}$, parallel to the tight-binding chain. Note that the form of this operator should be immaterial for the establishment of thermal equilibrium, which is only determined by the power spectrum. Indeed, we can check whether the detailed-balance condition is necessary for the system to reach thermal equilibrium. To that end, we use the operator in (17) within a Markov approximation for the correlation function, $c(t) \propto \delta(t)$. We have found that a steady state is approached that does not correspond to thermal equilibrium [28].

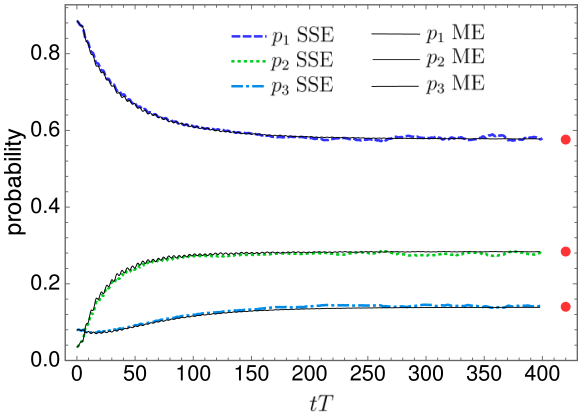

Figure 4. Dynamics of the occupation probabilities p_1, p_2, p_3 of the eigenstates of the Hamiltonian (16) in the one-electron sector calculated from the evolution of the TCLSSE (dashed lines) and the NMME (solid lines) with the power spectrum given by (15). The eigenstates are labeled such that the eigenenergies satisfy $\epsilon_1 \leq \epsilon_2 \leq \epsilon_3$. The red dots represent the thermal-equilibrium probabilities calculated from (18). The time t is measured in terms of the inverse of the energy constant T.

In figure 4 we show the occupation probabilities of the three eigenstates of the Hamiltonian in the one-electron sector as a function of time calculated using the TCLSSE (dashed lines) and the NMME (solid lines), respectively. For the TCLSSE, the results have been obtained by averaging over 90 000 independent realisations of the noise. We have used the parameters $\beta = 1$, $\omega_c = 1$, $T = 1$, $\epsilon_0 = 1$ and $\lambda = 0.1$ and we have employed the Euler algorithm [35, 36] with time step $\Delta t = 0.005$ to numerically solve the equations. As the establishment of thermal equilibrium is independent of the choice of the initial state, we have chosen an arbitrary pure state, $|\Psi(0)\rangle = 0.94\,|1\rangle + 0.2\,|2\rangle + 0.28\,|3\rangle$, where $|i\rangle$ represents the i-th eigenstate of the Hamiltonian, where the eigenenergies satisfy $\epsilon_1 \leq \epsilon_2 \leq \epsilon_3$.

The dynamics induced by the NMME and the TCLSSE are in good agreement: The small discrepancies in the numerical solutions are due to the finite number of realisations

we have used; the solution of the TCLSSE still contains some noise, as expected. For long times, both formalisms converge to the thermal-equilibrium probabilities

$$p_i = \frac{e^{-\beta\epsilon_i}}{e^{-\beta\epsilon_1} + e^{-\beta\epsilon_2} + e^{-\beta\epsilon_3}}. \tag{18}$$

If we were only interested in the long-time limit, we could have averaged over all times after some equilibration time $t_{\min}$ to obtain better statistics, using the ergodic theorem to replace the average over many realisations by an average over time of a single realisation.

3. Application to energy transport

To show that the TCLSSE can be used to investigate energy transport in open quantum systems, we consider a spin chain in contact with two baths at different temperatures. The baths are locally connected to the terminal spins of the chain [21, 37]. Energy is transferred between the high-temperature bath, via the spin chain, to the low-temperature bath. Here we assume the baths to be represented by an ensemble of harmonic oscillators with a continuous spectrum. In the long-time regime, we expect the appearance of a steady state of constant energy flow.

The total Hamiltonian of a spin-$1/2$ chain coupled to two baths L and R reads

$$\hat{H}_T = \hat{H}_S + \sum_{i=L,R} \big(\hat{H}_B^{(i)} + \hat{H}_{SB}^{(i)}\big), \tag{19}$$

where the system Hamiltonian is given by

$$\hat{H}_S = \frac{\Omega}{2} \sum_{\mu=1}^{n} \sigma_z^{(\mu)} + \Gamma \sum_{\mu=1}^{n-1} \vec{\sigma}^{(\mu)} \cdot \vec{\sigma}^{(\mu+1)}, \tag{20}$$

with $\vec{\sigma} = (\sigma_x, \sigma_y, \sigma_z)$ and the index μ indicating the spin site. The Pauli matrices are given by

$$\sigma_x = \begin{pmatrix} 0 & 1 \\ 1 & 0 \end{pmatrix}, \quad \sigma_y = \begin{pmatrix} 0 & -i \\ i & 0 \end{pmatrix}, \quad \sigma_z = \begin{pmatrix} 1 & 0 \\ 0 & -1 \end{pmatrix}. \tag{21}$$

Hence, the spin operators for the *n*-site chain are

$$\begin{array}{rccccccc} & & 1 & & 2 & & \mu & & n \\ \sigma_j^{(\mu)} = & \mathbb{1} & \otimes & \mathbb{1} & \otimes \cdots \otimes & \sigma_j & \otimes \cdots \otimes & \mathbb{1}. \end{array} \tag{22}$$

In (20), Ω is the energy associated with a uniform magnetic field aligned along the z direction and Γ is the spin-spin Heisenberg interaction.

The baths are coupled to the spins at the ends of the chain,

$$\hat{H}_{SB}^{(i)} = \lambda\, \hat{S}^{(i)} \otimes \hat{B}^{(i)} = \lambda\, \sigma_x^{(i)} \otimes \hat{B}^{(i)}, \tag{23}$$

where $\sigma_x^{(i=L)} = \sigma_x^{(1)}$, $\sigma_x^{(i=R)} = \sigma_x^{(n)}$, and λ is the coupling strength.

In line with (3), we need to assign the correlation function $c_{ab}(\tau)$. Here we use a bath correlation function describing the electromagnetic field of a one-dimensional cavity [5],

$$c^{(i)}(\tau) = \frac{\pi}{2\epsilon_0}\int_0^{\omega_c} d\omega\,\omega\left[\cos(\omega\tau)\,\coth\left(\frac{\beta^{(i)}\omega}{2}\right) - i\sin(\omega\tau)\right], \tag{24}$$

where $\beta^{(i)}$ is the inverse temperature of bath $i = L, R$. Accordingly, one can calculate the power spectrum of this bath correlation function as

$$C^{(i)}(\omega) = \frac{\pi^2|\omega|}{\epsilon_0}\left[n_B(\beta^{(i)}|\omega|) + \theta(-\omega)\right] \quad \text{for} \quad |\omega| < \omega_c. \tag{25}$$

This is the one-dimensional analogue of (15). One can immediately prove that this correlation function does fulfil the detailed-balance relation and therefore we expect the system to be driven towards thermal equilibrium if the temperatures of the two baths are the same.

To investigate the energy transport, we identify the energy current according to a continuity equation for the local energy. We define a local Hamiltonian according to

$$\hat{h}^{(\mu)} = \frac{\Omega}{2}\,\sigma_z^{(\mu)} + \frac{\Gamma}{2}\left(\vec{\sigma}^{(\mu)}\cdot\vec{\sigma}^{(\mu+1)} + \vec{\sigma}^{(\mu-1)}\cdot\vec{\sigma}^{(\mu)}\right) \tag{26}$$

if μ is different from n and 1.

We also define

$$\hat{h}^{(1)} = \frac{\Omega}{2}\,\sigma_z^{(1)} + \frac{\Gamma}{2}\,\vec{\sigma}^{(1)}\cdot\vec{\sigma}^{(2)} \tag{27}$$

and

$$\hat{h}^{(n)} = \frac{\Omega}{2}\,\sigma_z^{(n)} + \frac{\Gamma}{2}\,\vec{\sigma}^{(n-1)}\cdot\vec{\sigma}^{(n)} \tag{28}$$

so that $\hat{H}_S = \sum_\mu \hat{h}^{(\mu)}$. The time evolution of this local Hamiltonian is given by

$$-\frac{d\hat{h}^{(\mu)}}{dt} = -i\,[\hat{H}_S, \hat{h}^{(\mu)}] = \hat{j}^{(\mu),(\mu+1)} - \hat{j}^{(\mu-1),(\mu)}, \tag{29}$$

where energy-current operators have been defined as

$$\hat{j}^{(\mu),(\mu+1)} = \frac{i}{4}\left[\Omega\,(\sigma_z^{(\mu)} - \sigma_z^{(\mu+1)}),\ \Gamma\,\vec{\sigma}^{(\mu)}\cdot\vec{\sigma}^{(\mu+1)}\right]. \tag{30}$$

Equation (29) has the form of a continuity equation for the energy at site μ and is valid for sites inside the spin chains that are not coupled to a bath.

In figure 5 we report the energy current flowing from the second to the third spin of a three-site spin chain. In the equal-temperature case ($\beta^L = \beta^R = 5$, green solid and grey dashed lines in figure 5), a steady state is reached for long times that coincides with the thermal equilibrium and hence no current is flowing through the system. On the other hand, for the case of unequal temperatures ($\beta^L = 2$ and $\beta^R = 5$), the steady state shows a non-zero energy current from the warmer to the colder bath, as expected (black solid and red dot-dashed lines in figure 5). For the TCLSSE we have averaged over $100\,000$ independent realisations of the noise and for both calculations we have used the parameter values $\Omega = 1$,

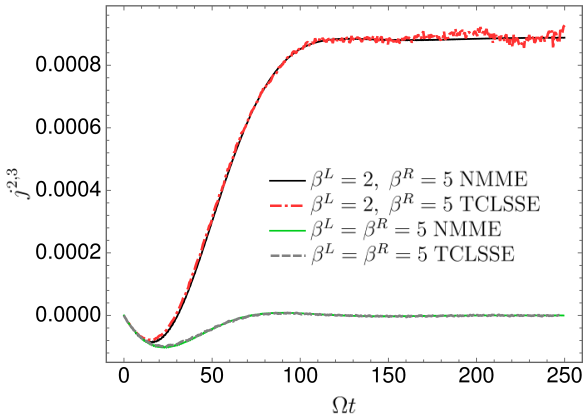

Figure 5. Dynamics of the energy current of a three-site spin chain coupled locally to two baths for the cases of equal and unequal temperatures, calculated with the NMME (solid lines) and the TCLSSE (dashed and dot-dashed lines). The agreement between the two sets of lines is excellent, in particular at short times. The time t is measured in terms of the inverse of the energy constant Ω.

$\Gamma = 0.01$, $\lambda = 0.1$, $\epsilon_0 = 1$ and $\omega_c = 6$. Both for the equal-temperature case and for the case with a thermal gradient, we have chosen an initial state populated with the probabilities determined by the equilibrium distribution at the lower temperature. It can been seen that the TCLSSE produces the same dynamics of the energy current as obtained from the NMME in the equilibrium and non-equilibrium regime and hence can be seen as a reliable tool to simulate energy transport with moderate numerical cost.

4. Conclusions

In conclusion, we have numerically investigated a time-local (time-convolutionless) version of a *non-Markovian* stochastic Schrödinger equation, which correctly describes the approach to thermal equilibrium and energy transport as obtained from the general master equation (2). We report two case studies, which show that the TCLSSE is a viable alternative for obtaining the exact dynamics of a non-Markovian open quantum system. Moreover, contrary to other approximations, e.g., the Born-Markov approximation to the Redfield equation [5], this stochastic equation reproduces the full dynamics of the non-Markovian master equation, and therefore could be used to investigate the transient dynamics and the approach to equilibrium. The TCLSSE can be integrated with moderate numerical cost, comparable to that of a Markovian system. It also shows more advantageous scaling with the number of states compared to the master equation, which is particularly useful for large systems. We have also introduced an efficient and portable numerical algorithm for the generation of the coloured complex noise necessary to solve the time-convolutionless stochastic Schrödinger equation. Our numerical algorithm is moderately faster than other available algorithms and requires only the power spectrum, $C(\omega)$, of the bath-correlation function as input.

Acknowledgments

R. B. and R. D'A. acknowledge support from MICINN (FIS2010-21282-C02-01 and PIB2010US-00652), the Grupos Consolidados UPV/EHU del Gobierno Vasco (IT-319-07) and ACI-Promociona (ACI2009-1036) and the financial support of the CONSOLIDER-INGENIO 2010 "NanoTherm" (CSD2010-00044). R. B. acknowledges financial support from IKERBASQUE, Basque Foundation for Science and the Ministerio de Educación, Cultura y Deporte (FPU12/01576). C. T. acknowledges financial support by the Deutsche Forschungsgemeinschaft, in part through Research Unit FOR 1154 "Towards Molecular Spintronics". R.D'A. acknowledges the support from the Diputacion Foral de Gipuzkoa via the grant number Q4818001B and is thankful for its hospitality to the Physics Department of the King's College London.

Appendix A. Derivation of the bath correlation function

In this section, we give a derivation of the bath correlation function for the coupling of the electromagnetic field in a three-dimensional cavity of volume V to an electronic system. In the dipole approximation, the interaction Hamiltonian is

$$\hat{H}_{\rm int} = -q \sum_i \hat{\vec{r}}_i \otimes \hat{\vec{E}}(t), \tag{A.1}$$

where q is the charge of an electron and $\hat{\vec{E}}$ is the electric field inside the cavity. The wavelength of the electromagnetic field is assumed to be large compared to the system size, hence $\hat{\vec{E}}$ is considered to be uniform in space. For simplicity, we suppose that each mode of the cavity has the same polarization direction, $\vec{u}$. Thus the second-quantized form of this interaction term is [38]

$$\hat{H}_{\rm int} = -q \sum_{l,p} \vec{u} \cdot \langle \psi_l | \hat{\vec{r}} | \psi_p \rangle \hat{\epsilon}_l^\dagger \hat{\epsilon}_p \otimes \sum_k i p_k \big(\hat{b}_k e^{-i\omega_k t} - \hat{b}_k^\dagger e^{i\omega_k t} \big) = \hat{S} \otimes \hat{B}, \tag{A.2}$$

where $\epsilon_l^\dagger$ creates an electron in the system in the state $|\psi_l\rangle$. These states form an orthonormal basis of the system Hamiltonian. The k-th field mode inside the cavity with frequency ω_k is created by $\hat{b}_k^\dagger$ and we define $p_k = \sqrt{\omega_k/(2V\epsilon_0)}$, where ϵ_0 is the dielectric constant. We note, by comparing (A.2) and (1), that the coupling is already written in the required bilinear form. From (A.2) we can immediately read off the form of the operators $\hat{S}$ and $\hat{B}$. After having assigned these coupling operators, one can calculate the bath correlation function

$$\begin{aligned} c(t,\tau) &= {\rm Tr}_B[\hat{\rho}_B^{\rm eq}\, \hat{B}(t)\, \hat{B}(\tau)] \\ &= -{\rm Tr}_B \left[\hat{\rho}_B^{\rm eq} \sum_{k,j} p_k p_j \big(\hat{b}_k e^{-i\omega_k t} - \hat{b}_k^\dagger e^{i\omega_k t} \big) \big(\hat{b}_j e^{-i\omega_j \tau} - \hat{b}_j^\dagger e^{i\omega_j \tau} \big) \right]. \end{aligned} \tag{A.3}$$

Evaluating the trace in the bosonic many-particle basis of the bath and replacing the sum over the bath modes ω_k by an integral over frequency yields

$$c(t,\tau) = \frac{1}{2\epsilon_0\pi^2}\int_0^{\omega_c} d\omega\,\omega^3\Big\{\big[n_B(\beta\omega)+1\big]\,e^{-i\omega(t-\tau)} + n_B(\beta\omega)\,e^{i\omega(t-\tau)}\Big\}, \tag{A.4}$$

where we have inserted the density of states in the cavity, ω^2/π^2. We have introduced a cutoff frequency ω_c to be consistent with the dipole approximation, which restricts the wavelengths of the bath modes to be larger than the system size. In addition, we note that the integral cannot be evaluated analytically, whereas the power spectrum of this function, (15), is analytically known.

References

[1] Einstein A 1905 *Ann. Phys. (N. Y.)* **322** 549
[2] Langevin P 1908 *C. R. Acad. Sci.* **146** 530
[3] Kloeden P E and Platen E 1999 *Numerical Solution of Stochastic Differential Equations* (Heidelberg: Springer-Verlag)
[4] Gardiner C W and Zoller P 2000 *Quantum Noise* 2nd ed (Berlin: Springer)
[5] Breuer H P and Petruccione F 2002 *The Theory of Open Quantum Systems* (New York: Oxford University Press)
[6] Razavy M 2006 *Classical and Quantum Dissipative Systems* (London: Imperial College Press)
[7] van Kampen N G 2007 *Stochastic Processes in Physics and Chemistry* 3rd ed (Amsterdam: Elsevier)
[8] Weiss U 2007 *Quantum Dissipative Systems* 3rd ed (Singapore: World Scientific)
[9] Ghirardi G C, Pearle P and Rimini A 1990 *Phys. Rev. A* **42** 78
[10] Diósi L and Strunz W T 1997 *Phys. Lett. A* **235** 569
[11] Gaspard P and Nagaoka M 1999 *J. Chem. Phys.* **111** 5676
[12] Yu T, Diósi L, Gisin N and Strunz W T 1999 *Phys. Rev. A* **60** 91
[13] Strunz W T, Diósi L and Gisin N 2000 *Lect. Notes Phys.* **538** 271
[14] D'Agosta R and Di Ventra M 2008 *Phys. Rev. B* **78** 165105
[15] Pershin Y V, Dubi Y and Di Ventra M 2008 *Phys. Rev. B* **78** 054302
[16] Marques M A L, Ullrich C A, Rubio A, Nogueira F, Burke K and Gross E K U (eds) 2006 *Time-Dependent Density Functional Theory* (*Lecture Notes in Physics* vol 706) (Berlin: Springer)
[17] Burke K, Car R and Gebauer R 2005 *Phys. Rev. Lett.* **94** 146803
[18] Di Ventra M and D'Agosta R 2007 *Phys. Rev. Lett.* **98** 226403
[19] Nakajima S 1958 *Prog. Theor. Phys.* **20** 948
[20] Zwanzig R 1960 *J. Chem. Phys.* **33** 1338; 1964 *Physica* **30** 1109
[21] Wichterich H, Henrich M, Breuer H P, Gemmer J and Michel M 2007 *Phys. Rev. E* **76** 031115
[22] Tokuyama M and Mori H 1976 *Prog. Theor. Phys.* **55** 411
[23] Hashitsume N, Shibata F and Shingū M 1977 *J. Stat. Phys.* **17** 155; Shibata F, Takahashi Y and Hashitsume N 1977 *J. Stat. Phys.* **17** 171
[24] Timm C 2011 *Phys. Rev. B* **83** 115416
[25] Strunz W and Yu T 2004 *Phys. Rev. A* **69** 052115
[26] de Vega I, Alonso D and Gaspard P 2005 *Phys. Rev. A* **71** 023812
[27] de Vega I, Alonso D, Gaspard P and Strunz W T 2005 *J. Chem. Phys.* **122** 124106
[28] Biele R and D'Agosta R 2012 *J. Phys. Condens. Matter* **24** 273201
[29] Łuczka J 2005 *Chaos* **15** 26107
[30] Rice S O 1944 *Bell Syst. Tech. J.* **23** 2
[31] Billah K Y R and Shinozuka M 1990 *Phys. Rev. A* **42** 7492
[32] Barrat J L and Rodney D 2011 *J. Stat. Phys.* **144** 679

[33] Koller S, Grifoni M, Leijnse M and Wegewijs M R 2010 *Phys. Rev. B* **82** 235307
[34] Mannella R and Palleschi V 1992 *Phys. Rev. A* **46** 8028
[35] Press W H, Teukolsky S A, Vetterling W T and Flannery B P 2001 *Numerical Recipes in Fortran 77: The Art of Scientific Computing* (Cambridge: Cambridge University Press)
[36] Kloeden P E, Platen E and Schurz H 1997 *Numerical Solution of SDE Through Computer Experiments* 3rd ed (Berlin: Springer-Verlag)
[37] Mejia-Monasterio C and Wichterich, H 2007 *Eur. Phys. J. Spec. Top.* **151** 113
[38] Schleich W P 2001 *Quantum Optics in Phase Space* (Berlin: Wiley-VCH)